

Highly Scalable, Uniform, and Sensitive Biosensors Based on Top-Down Indium Oxide Nanoribbons and Electronic Enzyme-Linked Immunosorbent Assay

Supporting Information

Noppadol Aroonyadet^{†‡}, Xiaoli Wang^{†‡}, Yan Song[‡], Haitian Chen[†], Richard J. Cote[§], Mark E. Thompson[‡], Ram H. Datar^{§}, and Chongwu Zhou^{†*}*

[†]Department of Electrical Engineering, [‡]Department of Chemistry, University of Southern California, Los Angeles, California 90089, United States. [§]Department of Pathology, University of Miami, Miami, Florida 33136, United States.

Corresponding Authors

*Email: chongwuz@usc.edu and rdatar@med.miami.edu

Materials 3" 500 nm SiO₂ on Si wafers and 4" Si wafers were purchased from SQI. LOL 2000 and 3612 photo resist were purchased from Shipley. Au and Ti for metal sources of electron beam evaporation and an indium oxide (In₂O₃) sputtering target with purity of 99.99% were obtained from Plasmaterials. 3-Phosphonopropionic acid with purity of 94 %, N-(3-Dimethylaminopropyl)-N'-ethylcarbodiimide hydrochloride (EDC) with purity of 98%, and N-Hydroxysuccinimide (NHS) with purity of 98 % were purchased from Sigma Aldrich. Streptavidin conjugated Alexar Fluor 568 was purchased from Life Technologies. Amine-PEG3-Biotin was purchased from Thermo Scientific. Amine PEG was purchased from Nanonocs. Streptavidin conjugated with 20 nm Au nanoparticles were purchased from Ted Pella. Human immunodeficiency virus 1 (HIV1) p24 monoclonal antibodies and HIV1 p24 proteins were purchased from Fitzgerald Industries. Biotinylated HIV1 p24 polyclonal antibodies were purchased from Abcam.

Device Fabrication 500 nm Si₃N₄ on Si wafers were deposited by low pressure chemical vapor deposition (LPCVD) system in Nanoelectronic Research Facilities (NRF), University of California at Los Angeles. After that, Si₃N₄/Si wafer was rinsed with acetone and isopropyl alcohol before dried in nitrogen stream before the fabrication process. After solvent cleaning, the Si₃N₄/Si substrate was placed on a hot plate at 120 °C for 5 minutes to repel all solvent residual and cool down in room temperature. After cleaning process and coating with bi-layered photoresist (LOL 2000 and SPR 3612 photoresist), source and drain electrodes were patterned using standard photolithography. O₂ plasma was treated at 60 W 50 mTorr for 18 s to remove thin layer of photoresist residual before metal deposition for better metal contact. Then, Ti/Au metal with 5/45 nm thickness were deposited by electron beam evaporation and lift-off process was used to remove unwanted areas. After coating with bi-layered photoresist, the

second mask was used to define nanoribbons by traditional photolithographic process. After nanoribbon patterning, O₂ discum was treated at 60 W 50 mTorr for 18 s to remove thin layer of photoresist residual before In₂O₃ sputtering. In₂O₃ nanoribbons were sputtered by Denton II sputtering system in NRF. After sputtering, unwanted In₂O₃ was removed by the lift-off process yielding the pristine surface.

Surface Functionalization After device fabrication, In₂O₃ nanoribbon FETs were submerged in boiling acetone and isopropyl alcohol for 5 minutes before dried in N₂ stream. To generate hydroxyl groups on the surface of In₂O₃ nanoribbon to accommodate phosphonic acid linker molecules, devices were treated by O₂ asher at 100 W 150 mTorr for 40 s. For biotinylated linker molecules, devices were incubated 1 mM biotinylated phosphonic acid in methanol for 5.5 hours. After biotinylated liker molecule incubation, devices were extensively rinsed with methanol. For the normal linker, devices were submerged in 1 mM aqueous solution of 3-Phosphonopropioninc acid for 5.5 hours before they were rinsed with deionized (DI) water to remove unbound linkers. After immobilization of linker molecules, devices were annealed at 120 °C in N₂ environment for 12 hours to dehydrate surface and to reinforce linkers on the In₂O₃ nanoribbon surface.

Anchoring of Amine Probe Molecules. After devices were functionalized with 3-Phosphonopropioninc acid linker, devices were treated with mixture of 20 mM EDC and 5 mM NHS in DI water for 1 hour to convert from carboxylic acid functional groups to NHS ester groups for covalently binding of amine molecules on the nanoribbon surface. After 1 hour, devices were rinsed with DI water before devices were incubated in solution of amine molecules (100 µg/ml of HIV1 p24 antibodies in 10 mM phosphate buffer saline (PBS) solution pH 7.4 for 4 hours at room temperature to allow amine functional groups to react with NHS ester functional groups on the nanoribbon surface.

Synthesis of Biotinylated Phosphonic Acid Linker The process started with synthesis of 6-(diethoxyphosphoryl)hexyl 5-(2-oxohexahydro-1H-thieno[3,4-d]imidazol-4-yl) pentanoate (product 1) as shown in Figure S1. A stirred solution of diethyl (6-hydroxyhexyl)phosphonate (0.952g, 4 mmole) in dry Dimethylformamide (DMF) (30 mL) was mixed with biotin powder (0.813g 3.3 mmole), EDC•HCl (766 mg, 4 mmole) and 4-Dimethylaminopyridine (DMAP) (488 mg, 4 mmole). The reaction mixture was stirred at room temperature under inert atmosphere for 2 hours and poured into water. The aqueous layer was extracted with ethyl acetate. The organic layer was washed with water, 1 M sodium hydroxide (NaOH) aqueous solution, 1 M hydrochloric acid (HCl) aqueous solution and brine, dried over Na₂SO₄ and concentrated *in vacuo* to give the crude oil. The crude residue was purified by flash chromatography (Dichloromethane/Methanol alcohol, DCM/MeOH, 10:1) to give the purified of product 1 (0.777g, 1.6 mmole, 50%).

Synthesis of (6-((5-(2-oxohexahydro-1H-thieno[3,4-d]imidazol-4-yl)pentanoyl)oxy) hexyl) phosphonic acid (product 2) started with a stirred solution of product 1 (0.1 g, 0.2 mmole) in dry DCM (10 mL). Bromotrimethylsilane (0.113 g, 0.75 mmole) was added into a stirred solution under inert atmosphere. The reaction mixture was stirred at room temperature for overnight and volatiles were evaporated *in vacuo*. 10 mL methanol was added into the residue and the mixture was stirred for 2 hours at room temperature. The reaction mixture was evaporated under *in vacuo* to give product 2 (quantitative) as a hygroscopic solid.

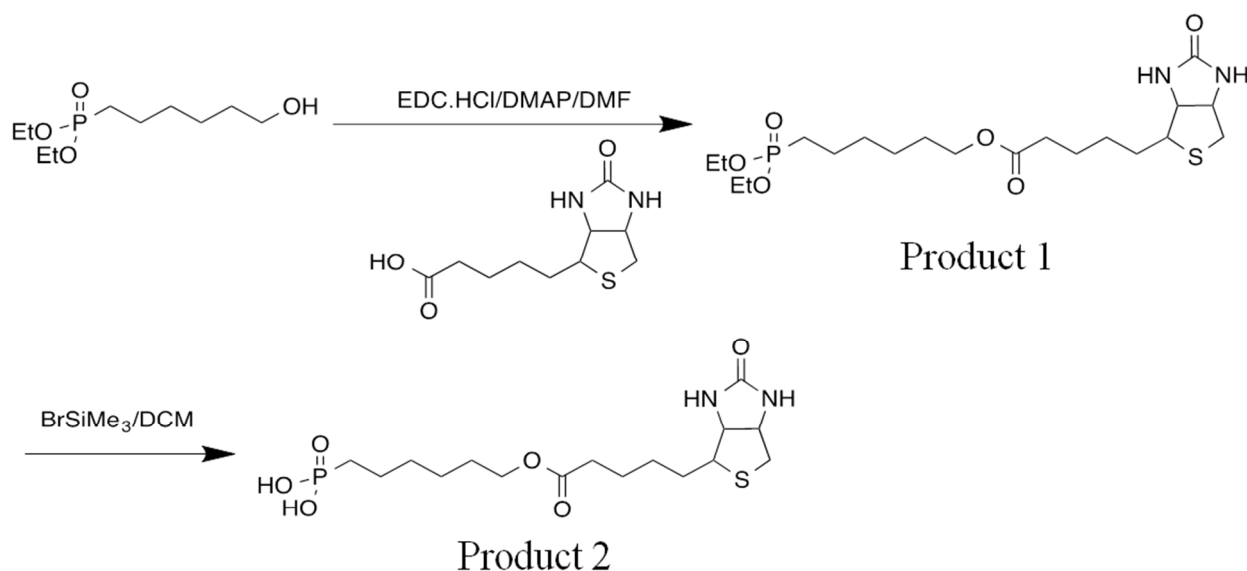


Figure S1. Schematic diagram of synthesis of biotinylated phosphonic linker molecule

In₂O₃ Nanoribbon Debye Length Calculation From I_{DS} - V_{DS} measurement in Figure 2a, total resistance (R) is calculated and approximate to be only channel resistance ($R = 40 \text{ M}\Omega$) due to a small value of contact resistance (R_C). From the nanoribbon structure, we have calculated (A/l) to be $2.67 \times 10^{-7} \text{ cm}$. Therefore, resistivity (ρ) is calculated from $\rho = R(A/l) = 10.8 \text{ }\Omega \cdot \text{cm}$. From average electron mobility (μ) of In₂O₃ nanoribbon devices shown in Figure 2d about $23.38 \text{ cm}^2/\text{V}\cdot\text{s}$, electron density (n) is calculated from $n = 1/(e\mu\rho) = 2.48 \times 10^{16} \text{ cm}^{-3}$ where e is electron charge in C. This yields λ_D to be approximate 23 nm.

Fluorescent Confirmation of Phosphonic Acid Chemistry Using Biotin-Streptavidin. Figure S6a and b show schematic diagrams of how fluorescent experiments were performed using biotin and dye-tagged streptavidin as the model probe-analyte system. The negative controls were anchored with amine polyethylene glycol (PEG) as probe instead of biotin. Streptavidin molecules only bind specifically to biotin while they will not react with amine-PEG molecules

and can be rinsed off. Figure S6c and d are schematic diagrams of a substrate and its optical image that we used in the fluorescent experiment, respectively. We deposited large In_2O_3 pads on metal electrodes for better optical visibility fabricated on 500 nm SiO_2 and 500 nm Si_3N_4 on Si substrates. Figure S6e and f show fluorescent images taken from In_2O_3 fabricated on SiO_2/Si substrates for sample and its negative control, respectively. Figure S6g and h show fluorescent images taken from In_2O_3 fabricated on $\text{Si}_3\text{N}_4/\text{Si}$ substrates for sample and its negative control, respectively. We observed strong red fluorescent signals from In_2O_3 pad on the metal electrodes from both samples on SiO_2/Si and $\text{Si}_3\text{N}_4/\text{Si}$ substrates confirming that we were successful to attach biotin as probe molecules to capture streptavidin molecules as shown in Figure S6e and g, respectively. The fluorescent signal from the SiO_2 substrate in Figure S6e shows comparable fluorescent brightness to ones from In_2O_3 pads while the fluorescent signal from the Si_3N_4 substrate in Figure S6g has much less fluorescent signal than one from In_2O_3 pads. Fluorescent images of their negative controls shown in Figure S6f and h, which were absence of biotin molecules, exhibited less streptavidin binding than their sample shown in Figure S6e and g, respectively. To increase sensitivity and lower limit of detection of our nanoribbon biosensor platform, Si_3N_4 on Si substrate is used in the device fabrication to reduce competition binding from the substrate of biosensors.

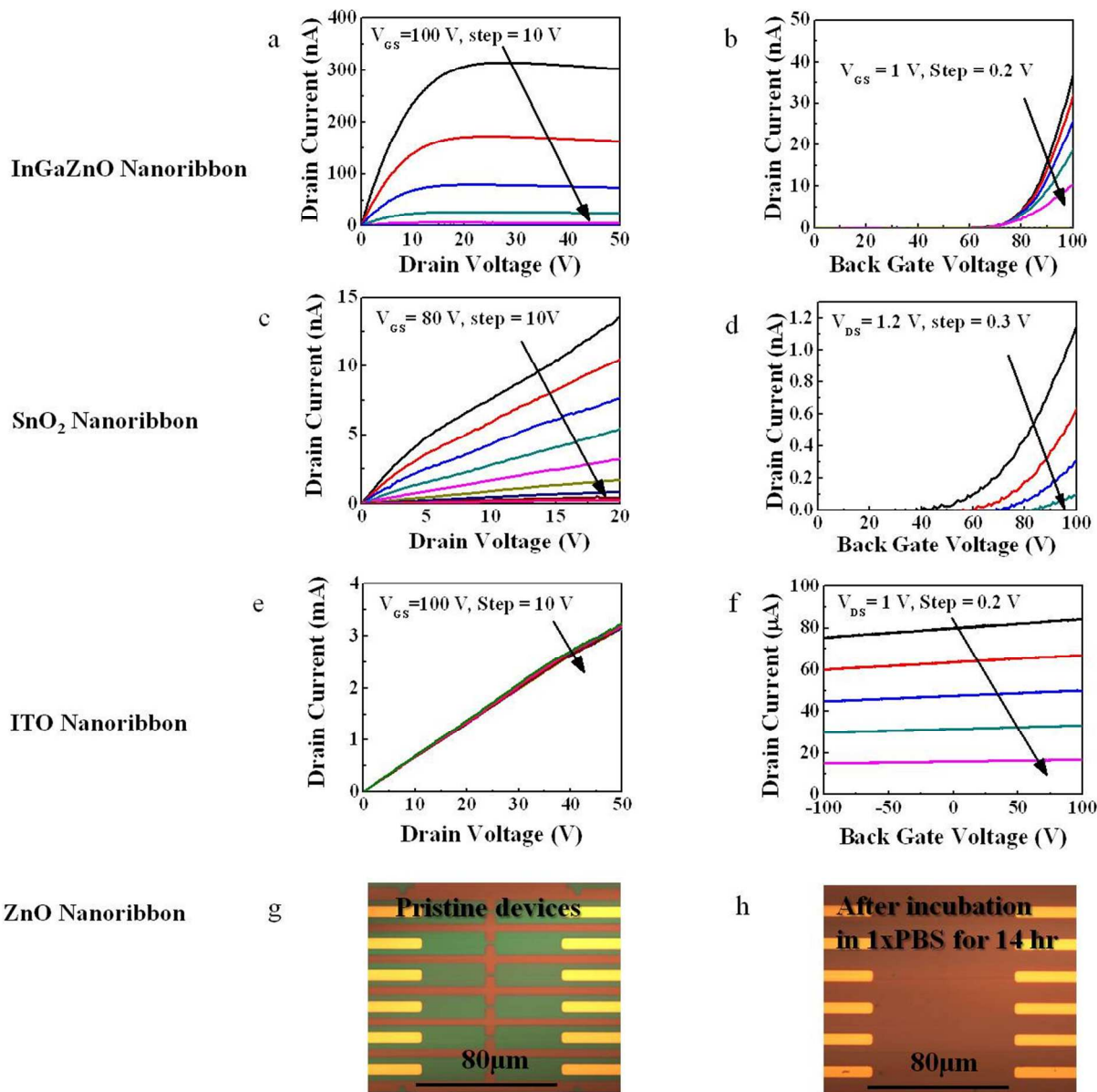


Figure S2. Families of I_{DS} - V_{DS} and I_{DS} - V_{GS} curves of (a, b) an InGaZnO nanoribbon device (c, d) a SnO₂ nanoribbon device (d, e) an ITO nanoribbon device at $V_{DS} = 200$ mV. Optical images of a ZnO nanoribbon device (g) before and (h) after 14 hour incubation in PBS. ZnO nanoribbons dissolved completely in PBS after 14 hours.

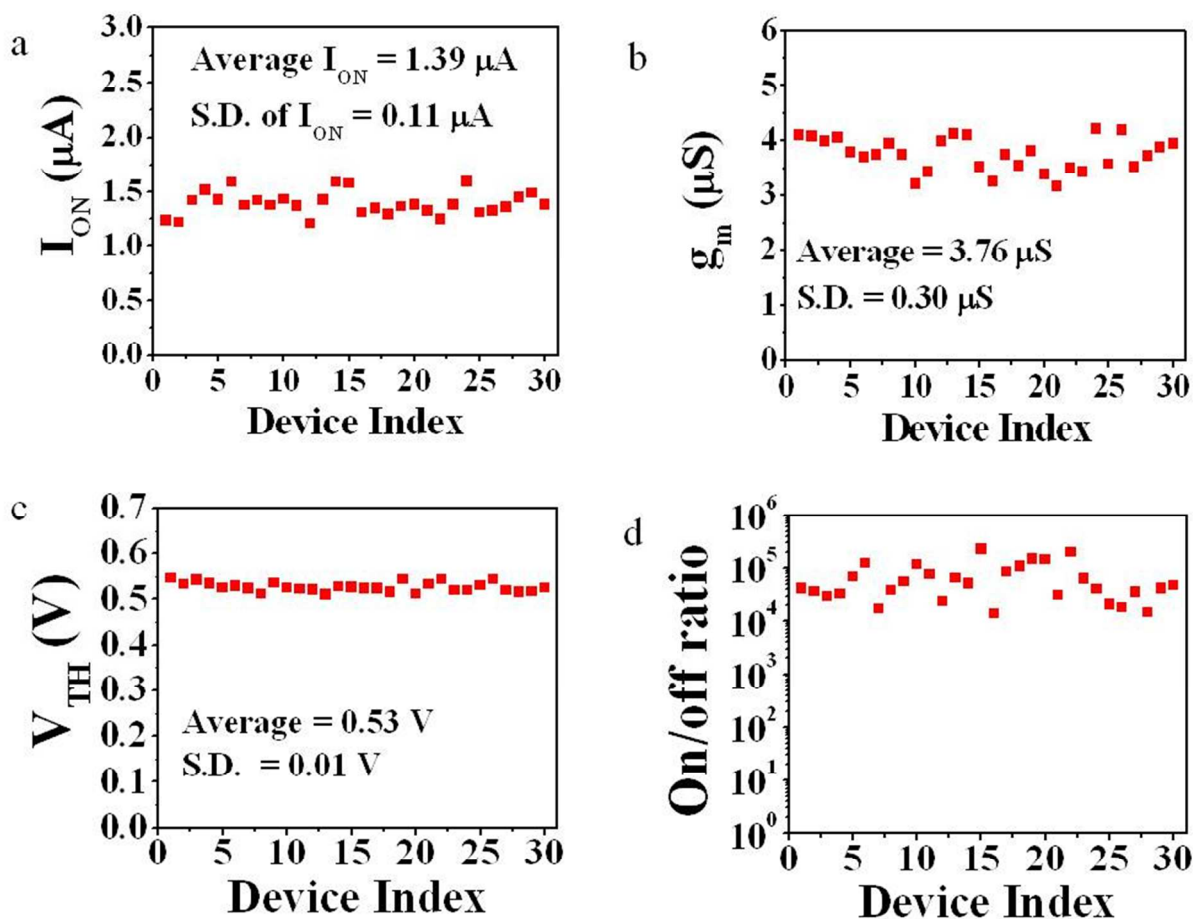


Figure S3. Distribution of electrical performance measured from 30 In_2O_3 nanoribbon devices in 0.01x PBS solution using a Ag/AgCl gate electrode. (a) On-state drain current (I_{ON}) at $V_{\text{DS}} = 200$ mV and $V_{\text{LG}} = 1$ V (b) Transconductance (g_m) at $V_{\text{DS}} = 200$ mV (c) Threshold voltage (V_{TH}) at $V_{\text{DS}} = 200$ mV and (d) On/off current ratios at $V_{\text{DS}} = 200$ mV.

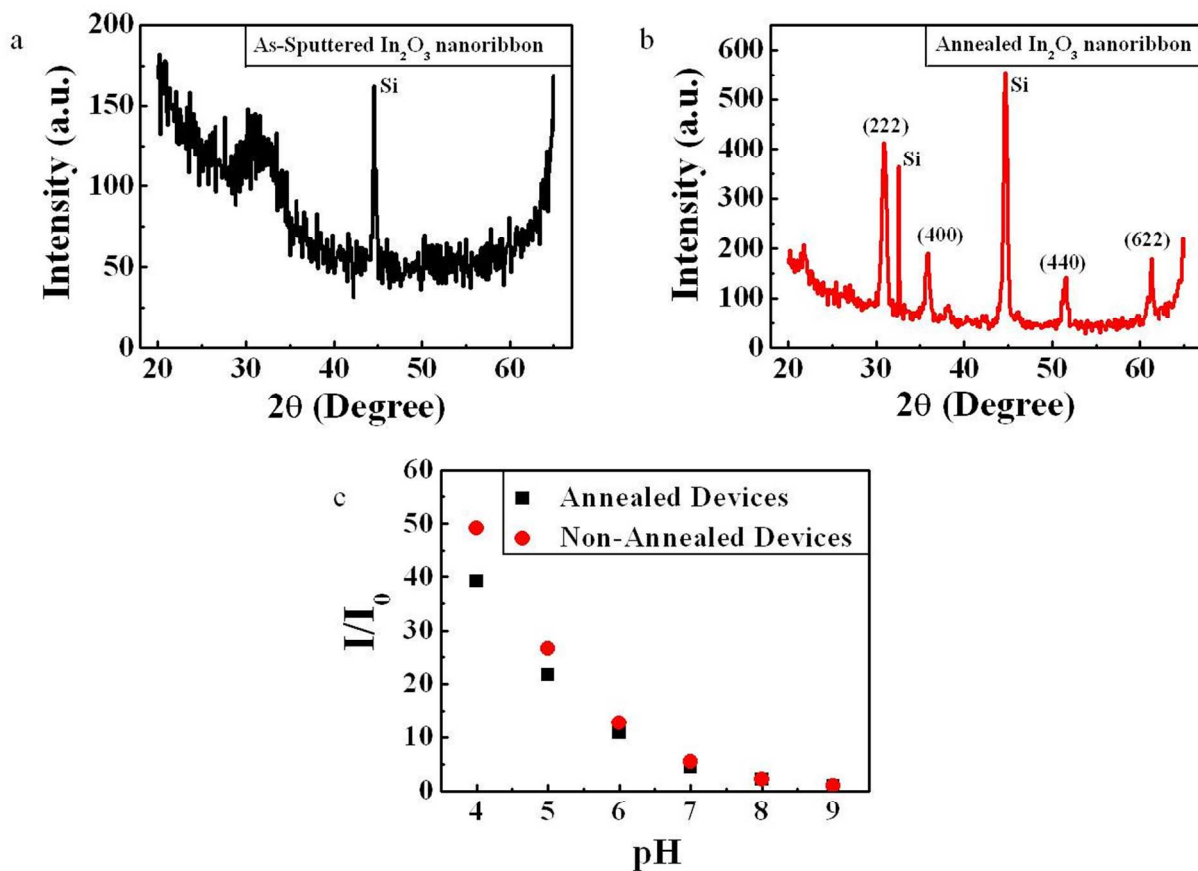


Figure S4. Plots from X-ray diffraction spectroscopy on 20 nm In_2O_3 film (a) Before annealing (b) After annealing in low vacuum at 300 °C for 30 minutes. (c) Comparison of average pH sensing responses obtained from three as-sputtered and annealed devices exposed to commercial pH buffer solutions with pH in a range of 4 to 9.

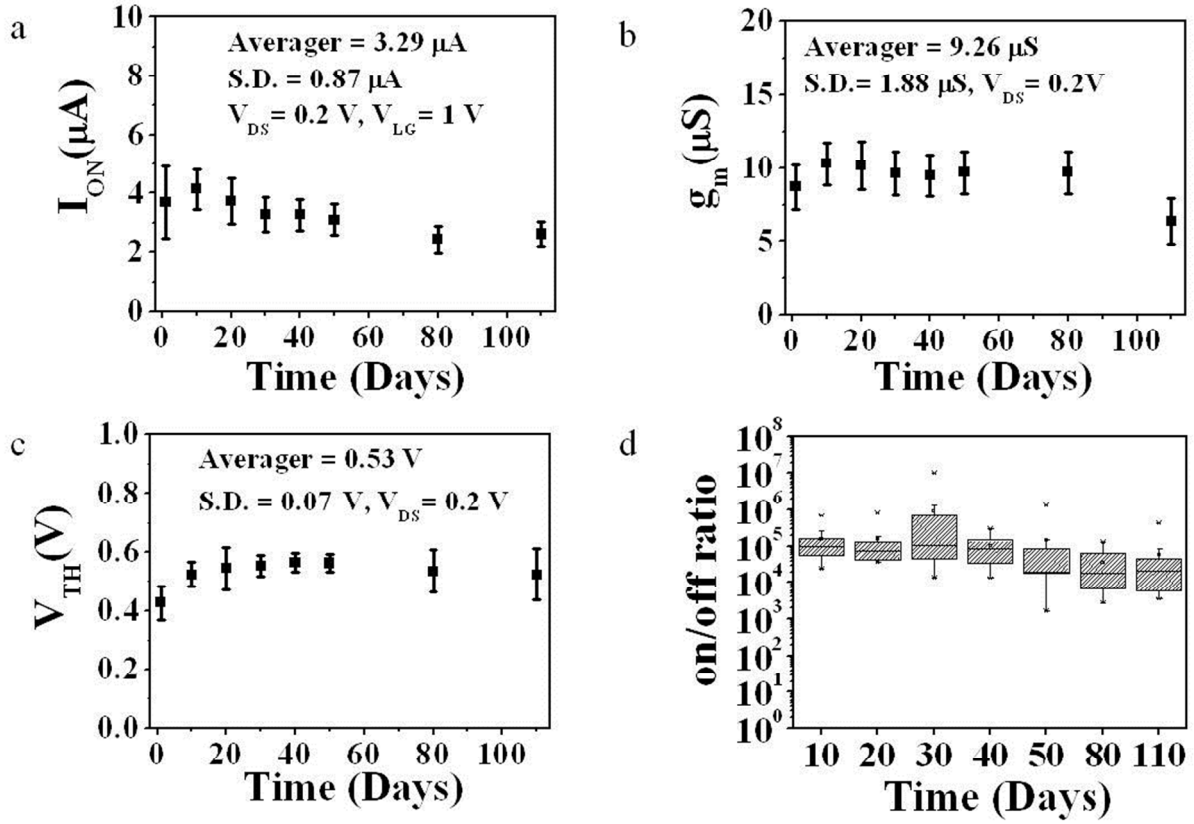


Figure S5. Key electrical performance parameters measured from 18 In_2O_3 nanoribbon devices immersed in 1x PBS at room temperature for the aqueous stability test (a) On-state current (I_{ON}) measured at $V_{\text{DS}} = 200 \text{ mV}$ and $V_{\text{LG}} = 1 \text{ V}$. (b) Transconductance (g_m) at $V_{\text{DS}} = 200 \text{ mV}$. (c) Threshold voltage (V_{TH}) at $V_{\text{DS}} = 200 \text{ mV}$. (d) On/off current ratio at $V_{\text{DS}} = 200 \text{ mV}$.

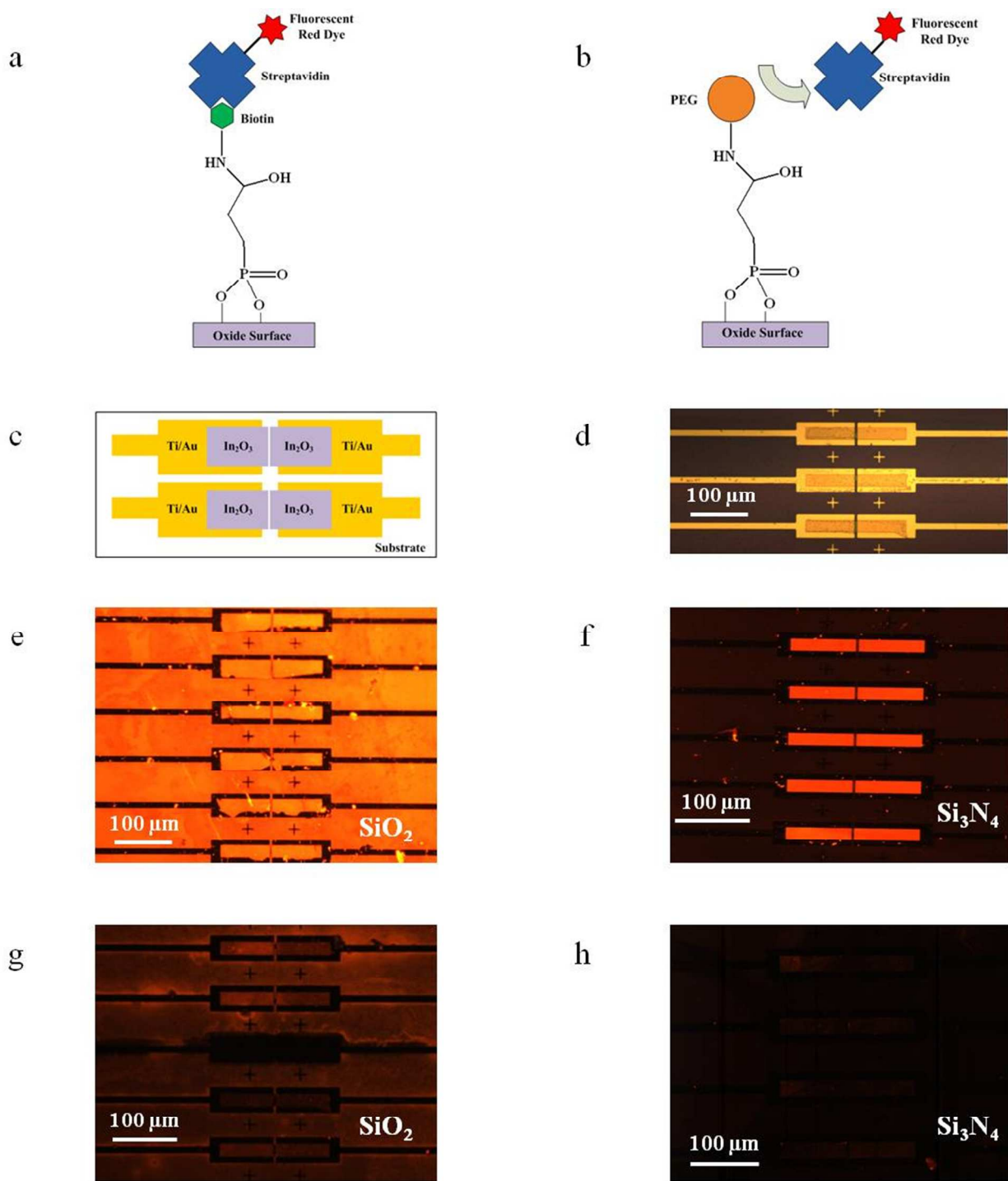


Figure S6. (a) A schematic diagram of a fluorescent sample functionalized with amine biotin to immobilize streptavidin conjugated with fluorescent red dyes. (b) A schematic diagram of fluorescent a negative control functionalized with amine PEG molecules which cannot bind with streptavidin conjugated with red fluorescent dyes. (c) A schematic diagram of In_2O_3 pads on Au

metal electrodes for fluorescent study (d) An optical image of In_2O_3 pads on Au electrodes for fluorescent experiment. Fluorescent images of (e) sample and (f) negative control of In_2O_3 pads fabricated on 500 nm SiO_2 on the Si substrate. Fluorescent images of (g) sample and (h) negative control of In_2O_3 pads fabricated on 500 nm Si_3N_4 on Si substrate.

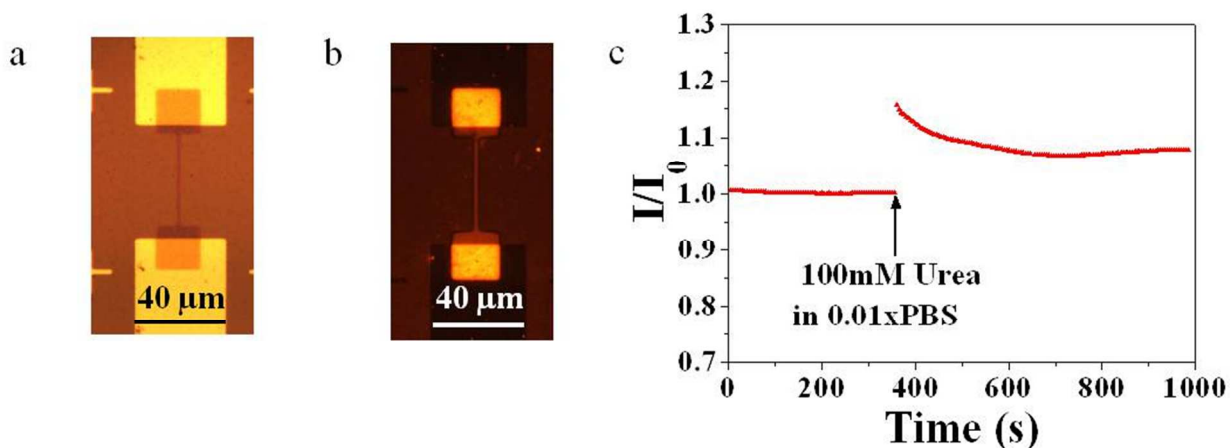


Figure S7. (a) An optical micrograph of an In_2O_3 nanoribbon (brown color) on Ti/Au metal electrodes after incubating with 1 μM streptavidin conjugated with red fluorescent dyes (b) A fluorescent image of the device in (a) to confirm binding of streptavidin molecules on an In_2O_3 nanoribbon having biotin capture probes (c) Real-time responses measured from an In_2O_3 nanoribbon device after incubating with streptavidin with fluorescent dyes without presence of urease enzymes in the sensing chamber. The device showed increase in conduction due to decrease in pH from 7.4 of 0.01xPBS to 6.61 of 100 mM urea in 0.01xPBS.

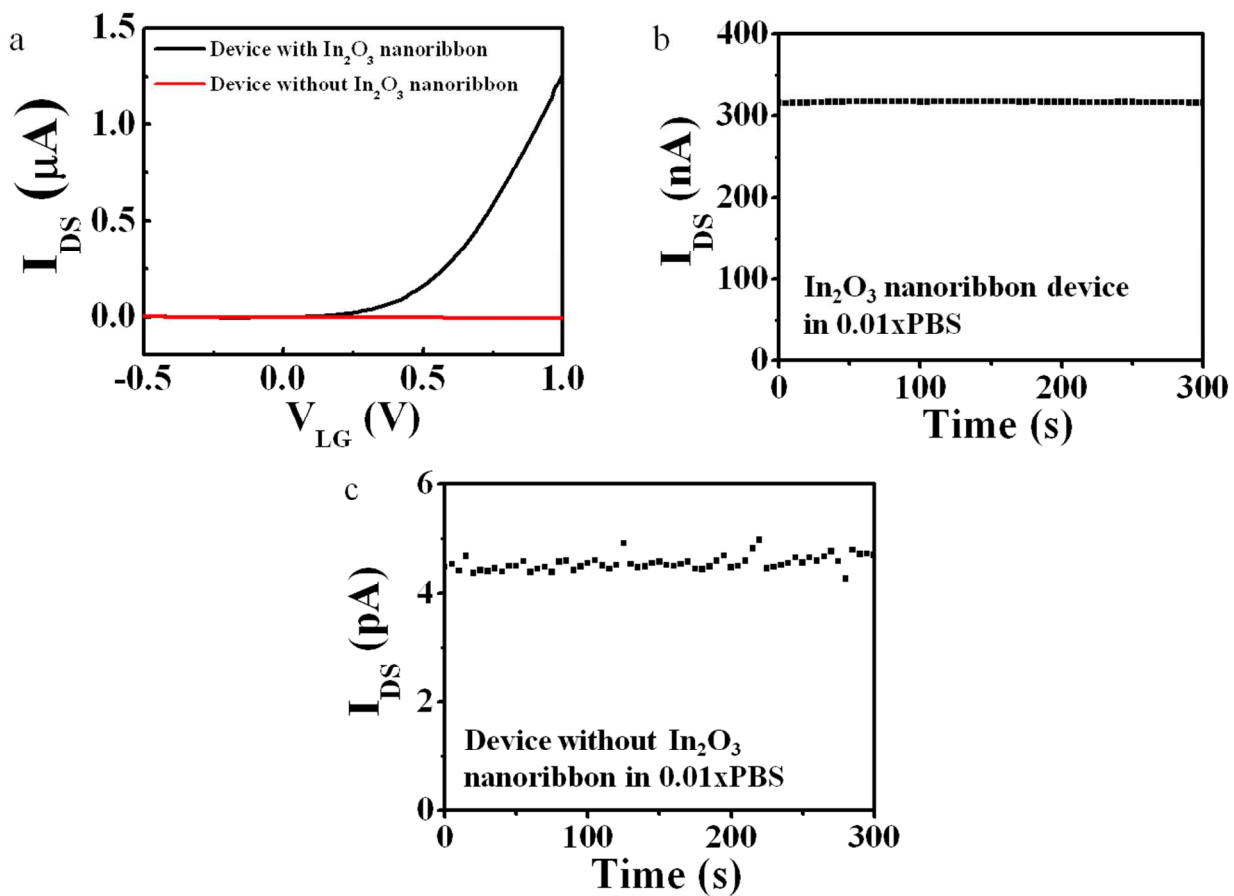


Figure S8. (a) Plots of drain current versus liquid gate voltage (I_{DS} - V_{LG}) measured from devices with and without In_2O_3 nanoribbon in 0.01xPBS. Plots of I_{DS} versus time measured from (b) an In_2O_3 nanoribbon device and (c) a device without In_2O_3 nanoribbon in 0.01xPBS.